BULLETIN OF THE POLISH ACADEMY OF SCIENCES
TECHNICAL SCIENCES, Vol. 68, No. 3, 2020
DOI: 10.24425/bpasts.2020.133368

Influence of process-material conditions on the structure and biological properties of electrospun polyvinylidene fluoride fibers

A. ZASZCZYŃSKA[1]*, P.Ł. SAJKIEWICZ[1], A. GRADYS[1], R. TYMKIEWICZ[2], O. URBANEK[1], and D. KOŁBUK[1]

[1] Institute of Fundamental Technological Research, Polish Academy of Sciences, Laboratory of Polymers and Biomaterials, Pawińskiego 5B, 02-106 Warsaw, Poland
[2] Institute of Fundamental Technological Research, Polish Academy of Sciences, Department of Ultrasound, Pawińskiego 5B, 02-106 Warsaw, Poland

Abstract. Polyvinylidene fluoride (PVDF) is one of the most important piezoelectric polymers. Piezoelectricity in PVDF appears in polar β and γ phases. Piezoelectric fibers obtained by means of electrospinning may be used in tissue engineering (TE) as a smart analogue of the natural extracellular matrix (ECM). We present results showing the effect of rotational speed of the collecting drum on morphology, phase content and in vitro biological properties of PVDF nonwovens. Morphology and phase composition were analyzed using scanning electron microscopy (SEM) and Fourier-transform infrared spectroscopy (FTIR), respectively. It was shown that increasing rotational speed of the collector leads to an increase in fiber orientation, reduction in fiber diameter and considerable increase of polar phase content, both β and γ. In vitro cell culture experiments, carried out with the use of ultrasounds in order to generate electrical potential via piezoelectricity, indicate a positive effect of polar phases on fibroblasts. Our preliminary results demonstrate that piezoelectric PVDF scaffolds are promising materials for tissue engineering applications, particularly for neural tissue regeneration, where the electric potential is crucial.

Key words: scaffolds, electrospinning, polyvinylidene fluoride, tissue engineering.

1. Introduction

As regards the field of biomedical engineering, in recent decades, increasing scientific and technical interest has been observed in research related to development of composites [1] and hydrogels [2] as well as the design of polymers with nanofillers [3, 4] and smart materials [5]. Smart materials are generally designed to react in response to external stimuli (physical, chemical, mechanical) thus behaving similar to natural body tissues [6–8]. One type of such smart materials are piezoelectric scaffolds, which can generate electrical signals in response to the applied stress or vice versa, constituting sensitive mechano-electrical transduction systems. It is anticipated that such materials can effectively stimulate signaling pathways and thereby enhance tissue regeneration at the impaired site. Piezoelectric phenomena are observed in animal bodies, for example in DNA, the tendons, bones, skin, cartilage, ligaments and the dentin.

It is known that electrical charges are important for the activity of cells, particularly neural cells. The major advantage of piezoelectric scaffolds is that electrical potential can be generated non-invasively under the influence of a mechanical field, without the need to use invasive electrodes. State-of-the-art in tissue engineering is directed towards minimally invasive and "smart" technologies [9–13]. In these approaches, smart materials are reported to help avoid complex and long surgeries.

Since the discovery of strong piezoelectric activity in polyvinylidene fluoride (PVDF), intensive research has been conducted on this polymer. At least four different polymorphs, referred to as α, β, γ, and δ phases, depending on the processing conditions, have been reported [14, 15]. Among them, the β-phase, showing the highest piezoelectricity because of trans-trans molecular conformation in orthorhombic crystals, has been reported during the past 40 years in numerous works aiming at high level of β-phase (Fig. 1) [16].

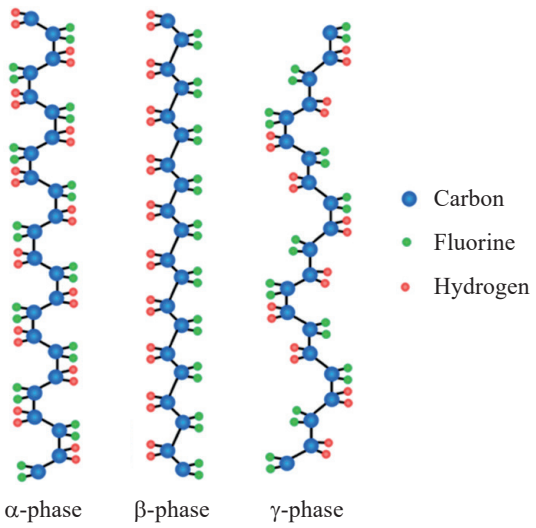

Fig. 1. Schematic representation of the chain conformation for the α, β and γ phases of PVDF

*e-mail: azasz@ippt.pan.pl

Manuscript submitted 2019-10-08, revised 2020-02-25, initially accepted for publication 2020-02-25, published in June 2020

A variety of experimental techniques, such as mechanical stretching [17], application of high pressure [18, 19], melt-quenching [20], poling under high electric field [21] and incorporating some additives (e.g. nanoparticles, nanowires, graphene) [22–26], have been investigated to induce formation of the β-phase. For piezoelectric applications, β-crystal samples must be subjected to a poling procedure to orient the CF_2 dipoles; however, they are more prone to break down under a high-electric field [27]. The presence of polar phases is very important, in particular, due to its bioelectrical effect in stimulation of the nervous system, holding promise of effective tissue regeneration [28–32]. The content of polar phases in nanofibers may also be affected by rotational speed of the collector used during electrospinning [33].

An interesting idea, reported only in few publications, is to design an innovative smart electrospun active piezoelectric scaffold for tissue engineering applications. Among polymeric materials, PVDF nanofibers have the strongest piezoelectric properties with practically no aging of piezoelectricity at the body temperature of mammals [34], rendering it biologically very attractive [35–38].

We recall the studies on the effect of rotational speed of the collecting drum on phase content, morphology and in vitro biological properties of PVDF nonwovens.

2. Materials and methods

2.1. Materials. Polyvinylidene fluoride (PVDF) nonwovens were formed using the electrospinning process from a mixture of acetone and an N,N′-dimethylformamide (DMF) solution. PVDF pellets (Kynar, $M_W = 400{,}000$ g/mol) were purchased from Arkema while high purity acetone and DMF were obtained from Merck.

Solutions of PVDF at the concentrations of 17, 19 and 22 (w/v%) were prepared by dissolving PVDF pellets in the DMF/acetone mixture of solvents at a 4:1 ratio. First, PVDF pellets were dissolved in DMF for 4 hours at 70°C, then acetone was added and the solution was mixed for 2h at room temperature to receive a homogeneous solution.

2.2. Electrospinning process. The electrospinning setup (Fig. 2) consisted of a syringe ended with a 0.3 mm needle facing a grounded rotating drum collector (4 cm radius and 12 cm in length). A high voltage generator with a positive terminal was connected to the stainless steel needle. The distance between the needle and the collector was 180 mm, flow rate of the solution was 600 µl/h. The applied voltage was in the range of 16–18 kV, which was optimum for obtaining uniform fibers and for maintaining a stable electrospinning process. Collecting of the fibers was performed at three rotational speeds of the collector: 100, 900 and 1000 rpm. The electrospinning process was conducted horizontally. After electrospinning, nonwovens were placed under a fume hood for 48 hours to remove solvent residue.

Samples were labeled with collector rotational speed and, if necessary, additional information was provided in the text or in the descriptions of figures.

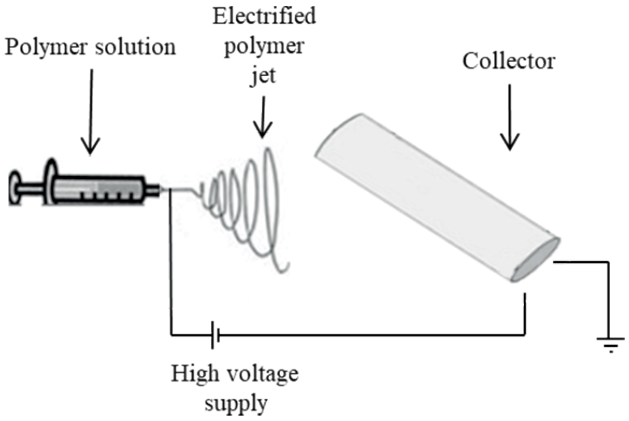

Fig. 2. Scheme of conventional electrospinning setup used with a rotating collector

2.3. Solution viscosity measurements. Solution viscosity was measured using a Brookfield HADV-III Ultra rotational viscometer with cone-plate configuration. In addition to the viscosity measurements at various shear rates, viscosity measurements at a constant shear rate ≈ 33 1/s were performed as a function of time during solution preparation in order to determine stability of the solution. The shear rate ≈ 33 1/s corresponds to the value estimated for the shear rate, inside the applied needle (1):

$$\gamma = \frac{4Q}{\pi r^3} \tag{1}$$

where Q is the volumetric flow rate (600 µL/h) and r is the inner needle radius (0.17 mm).

2.4. Scanning electron microscopy. Scanning electron microscopy (SEM) imaging was performed using scanning electron microscopy (SEM, Jeol JSM-6010PLUS/LV InTouchScope™) in order to determine the distribution of fiber orientation and diameter as a function of collector rotational speed. Before imaging, the nonwovens were coated with gold. The acceleration voltage was 10 kV. Data analysis was performed using ImageJ software. The fibers diameter distribution was determined by means of 100 measurements for each sample, using Gaussian function approximation. The fibers orientation distribution was determined using ImageJ software with a Directionality plugin. Half width was calculated using Pearson VII function for approximation of orientation distribution.

2.5. Fourier-transform infrared spectroscopy (FTIR). Fourier-transform infrared (FTIR) analysis was performed using the Perkin Elmer FTIR-ATR 100 instrument, MA, USA, and the data presented are representative of three independent samples and runs. The samples were scanned from 400 to 4000 cm^{-1} with a resolution of 2 cm^{-1} and a total of 32 scans.

The relative fraction of two polar phases, β and γ, in addition to non-polar α was determined according to the procedure

described in [38]. This method allows to determine relative amounts of the electroactive β and γ phases, F_{EA}, in terms of crystalline components in any samples such as a sample containing two phases ($\alpha+\beta$, $\alpha+\gamma$, or $\beta+\gamma$) or three phases ($\alpha+\beta+\gamma$):

$$F_{EA} = \frac{I_{840^*}}{\left(\frac{K_{840^*}}{K_{763}}\right) I_{763} + I_{840^*}} \times 100\% \tag{2}$$

where, characteristic absorption I_{840^*} and I_{763} are bands at 837–841 cm^{-1}, which can be assigned to both β and γ phases, and at 763 cm^{-1} attributed to an α phase, respectively, assuming these absorption bands follow the Beer-Lambert law with absorption coefficients of $K_{763} = 6.1\times10^4$ and $K_{840^*} = 7.7\times 104$ cm^2 mol^{-1}.

Quantification of individual β and γ phases content, F(β) and F(γ), was performed by using the absorbance (peak area or peak height) of the two bands at 1275 and 1234 cm^{-1}. However, a much more preferable method is proposed by calculating the peak-to-valley height ratio between the peaks around at 1275 and 1234 cm^{-1} and their nearest valleys:

$$F(\beta) = F_{EA} \times \left(\frac{\Delta H_{\beta'}}{\Delta H_{\beta'} + \Delta H_{\gamma'}}\right) \times 100\% \tag{3}$$

$$F(\gamma) = F_{EA} \times \left(\frac{\Delta H_{\gamma'}}{\Delta H_{\beta'} + \Delta H_{\gamma'}}\right) \times 100\% \tag{4}$$

where, $\Delta H_{\beta'}$ and $\Delta H_{\gamma'}$ are the height differences (absorbance differences) between the peak present at 1275 cm^{-1} and the nearest valley present at 1260 cm^{-1}, and the peak present at 1234 cm^{-1} and the nearest valley present at 1225 cm^{-1}, respectively.

2.6. Cellular studies. Polyvinylidene fluoride (PVDF) nanofibers were subjected to in vitro cellular studies. In the stimulation experiments, L929 fibroblast cells cultured on piezoelectric PVDF scaffolds, collected at various rotational speeds of the collector, were exposed to ultrasounds for 30 minutes, once a day, for 7 days. Ultrasound stimulus with the power of 20 mW/cm^2 and 80 mW/cm^2 at the frequency of 1.7 MHz was applied (Fig. 3). In order to confirm the piezoelectric effect of the PVDF scaffolds on fibroblasts activity, piezoelectric PVDF scaffolds without ultrasonic stimulation were used as a control (0 mW/cm^2) and a fibroblasts mitochondrial activity (MTT) test was conducted.

Observations of cell morphology on fibers were conducted using SEM.

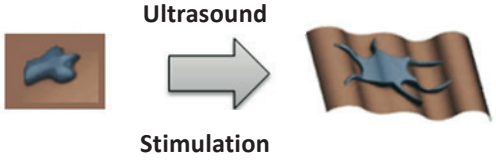

Fig. 3. Schematic illustration of the influence of ultrasound stimulation on the shape of L929 fibroblast cell

3. Results

3.1. Solution viscosity measurements. One of the most important material parameters of electrospinning is viscosity. It defines the resistance of the fluid to flow, thus stabilizing the jet. Viscosity is directly proportional to the concentration of the solution and to the molecular weight of the polymer.

From shear rate dependence in Fig. 4, it is evident that the shear thinning effect is seen only for the highest solution concentration, while for the lower concentrations the solutions behave like Newtonian fluids. The shear thinning effect is most probably related to an effective molecular orientation at higher shear rates. From the viscosity over time dependence (Fig. 5),

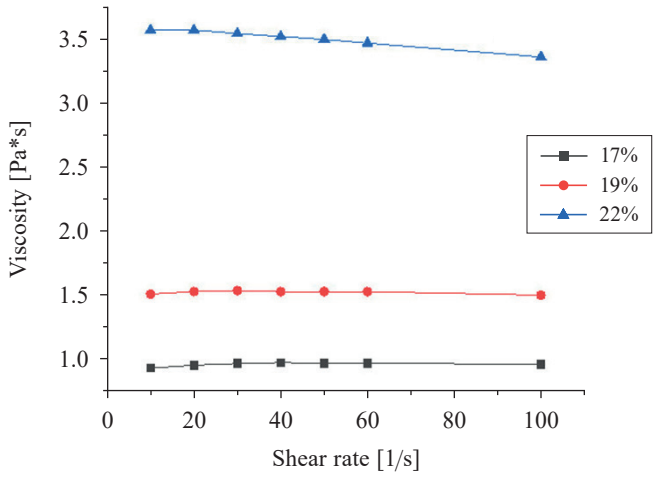

Fig. 4. Viscosity as a function of shear rate for various PVDF concentrations

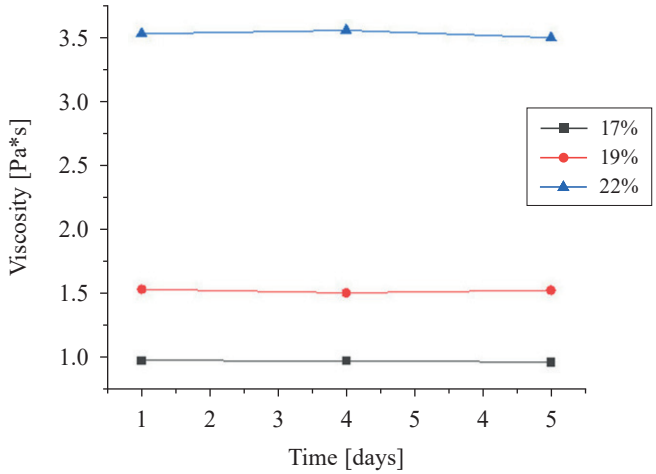

Fig. 5. Viscosity as a function of time (at shear rate = 33 1/s) for various PVDF concentrations

measured from the moment of solution preparation, it is seen that irrespective of the polymer concentration used, the solution is stable over time.

3.2. Electrospinning and morphology of fibers. All PVDF concentrations provided a stable electrospinning process, however, beadless fibers were obtained only for PVDF concentration of 22%. This solution was subjected to further studies.

In Figs. 6–8, SEM images and fiber diameter and orientation distribution for various collector rotational speeds are presented. The fiber diameter was in the range from 200 nm to 1.4 μm with the average value of 900 nm. It is seen that the average fiber diameter decreases with collector rotational speed, which is consistent with the previous results [39–44].

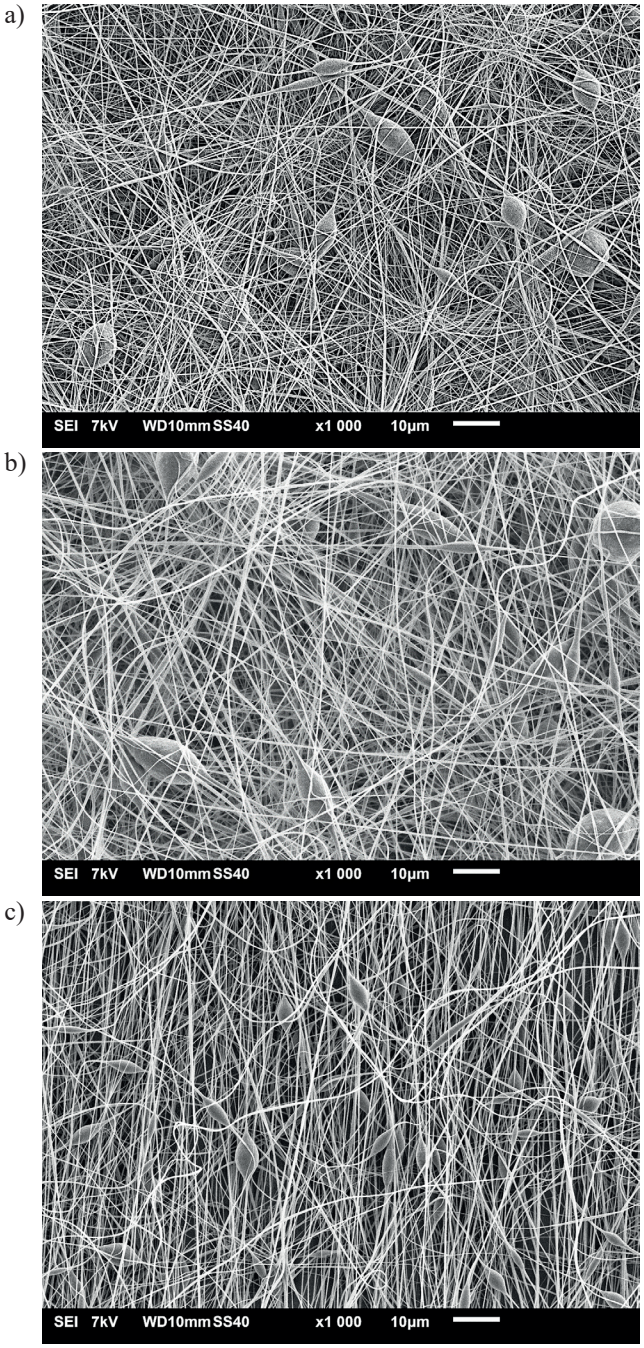

Fig. 6. SEM micrograph for nonwovens electrospun from 22% PVDF solution for different rotational speeds of the collector: a) 100 rpm, b) 900 rpm and c) 1000 rpm

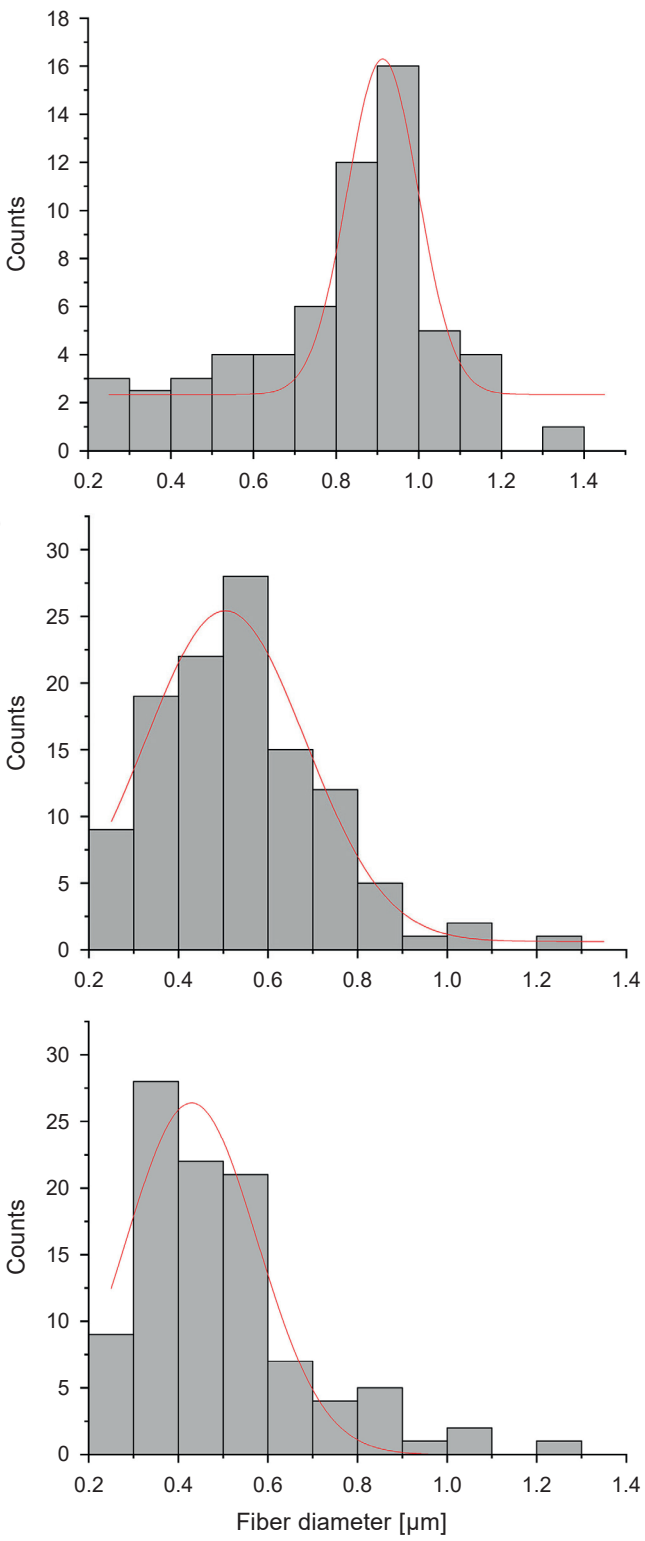

Fig. 7. Diameter distributions for nonwovens electrospun from 22% PVDF solution for different rotational speeds of the collector: a) 100 rpm, b) 900 rpm and c) 1000 rpm

This reduction is due to increasing tangential force caused by the rotating collector providing stronger mechanical stretching. From Fig. 8, it is evident that with increasing rotational speed, the fiber orientation distribution becomes narrower. The half width of the orientation distribution changes from 14.3° at 1000 rpm through 19.0° at 900 rpm to 86.1° at 100 rpm. Alignment around 90° in samples PVDF900 and PVDF1000 corresponds to the collector rotation direction.

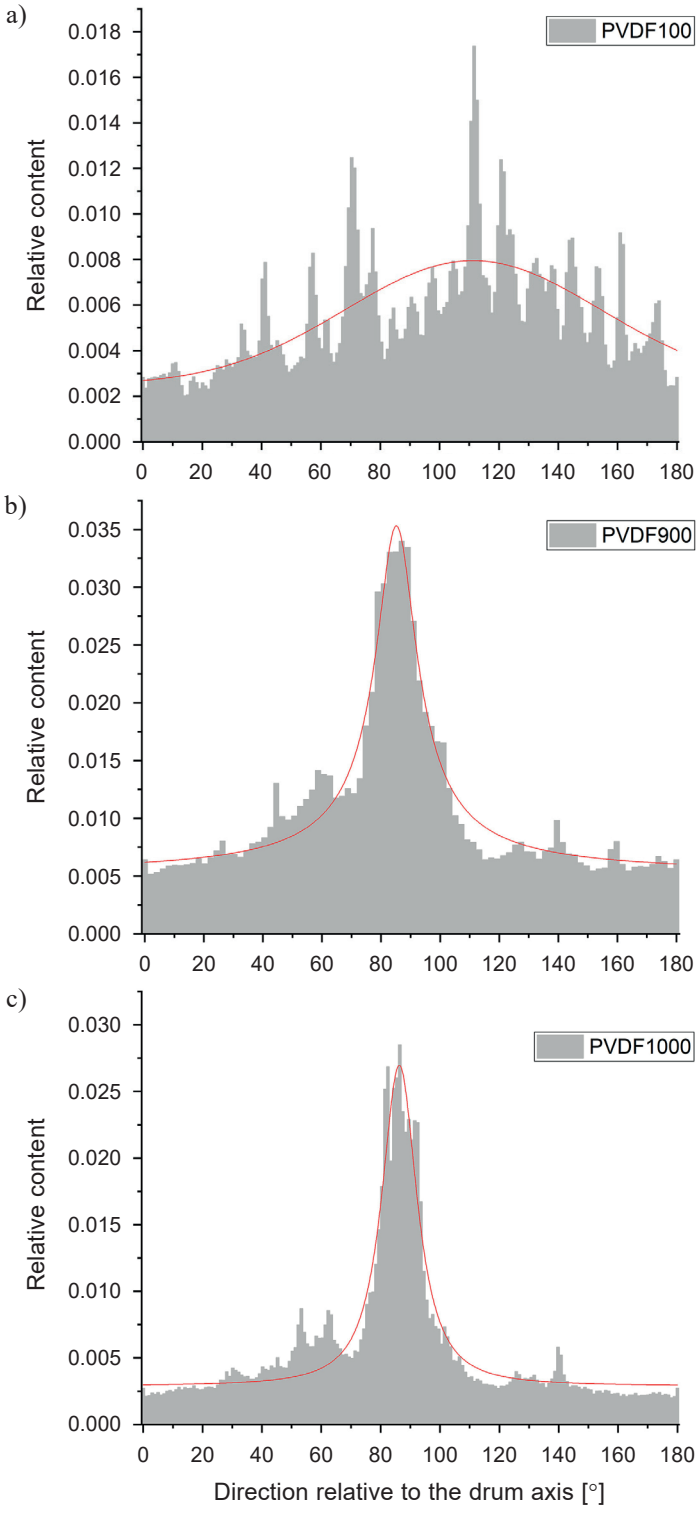

Fig. 8. Fiber orientation distribution (experimental data with numerical approximation) for nonwovens electrospun from 22% PVDF solution for different rotational speeds of the collector a) 100 rpm, b) 900 rpm and c) 1000 rpm

3.3. Fourier-transform infrared spectroscopy (FTIR). FTIR spectrum of PVDF nanofiber mats is shown in Fig. 9. Based on Equations (2–4), the relative fraction of the electroactive β and γ phases for all samples was calculated (Table 2). The randomly oriented electrospun PVDF fibers contain only 0.6% of polar phases, thus the piezoelectric effect should be negligible. At rotational speed of the collector of 900 and 1000 rpm, polar phases content is found at 76.65% and 94.48%, respectively. Thus, increasing collector rotation speed results not only in increased fiber orientation and smaller fiber diameter but also in a dramatic increase of the polar phase content.

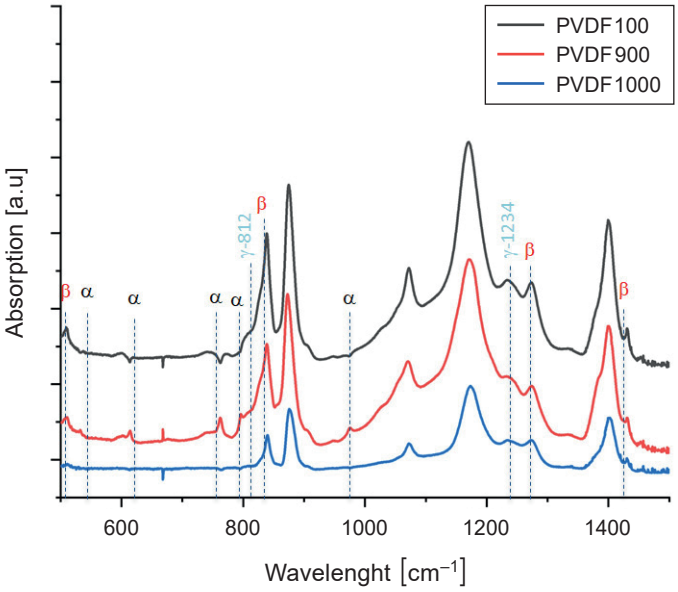

Fig 9. FTIR-ATR spectra for nonwovens spun from 22% PVDF solution. Most significant peaks corresponding to α-, β- and γ-phases are indicated

Table 2.
Relative content of polar phases in e-spun PVDF

Sample	$(F(\beta)+F(\gamma))$	$F(\beta)$	$F(\gamma)$
	[%]	[%]	[%]
PVDF100	0.60 ± 0.01	0.57 ± 0.01	0.03 ± 0.01
PVDF900	76.65 ± 0.2	72.03 ± 0.2	4.61 ± 0.2
PVDF1000	94.48 ± 0.2	55.17 ± 0.2	39.31 ± 0.2

3.4. Cellular studies. Results of MTT tests presented in Fig. 10 indicate a positive effect of polar phases on the cells via the piezoelectric effect achieved under ultrasounds stimulation. Cell viability results were in agreement with other studies that conclude that PVDF is not cytotoxic and that it allows cell

proliferation [24, 25]. Piezoelectric effect was mostly evident for samples formed at the highest collector rotational speed, allowing formation of the highest content of polar phases. The observations using SEM confirm good attachment and proliferation of the cells on the ultrasound-stimulated fiber scaffolds: on day 1, the cells had more rounded morphology, while by day 7, their morphology was more elongated and spread-out (Fig. 10).

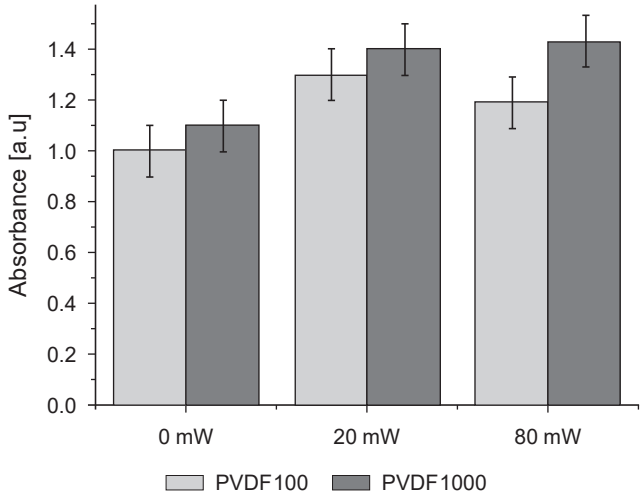

Fig. 10. Viability of L929 fibroblasts on PVDF100 and PVDF1000 samples using ultrasound stimulation with different power on day 7

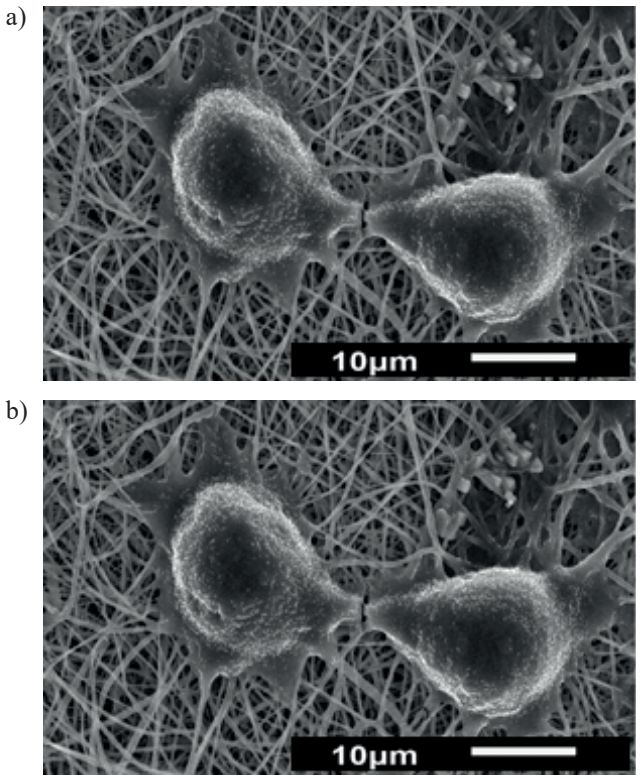

Fig. 11. SEM images of L929 fibroblasts on PVDF1000 nanofibers with power 80 mW/cm^2 a) on day 1 and b) on day 7

4. Conclusions

We showed that the application of relatively high rotational speed of the collector allows for electrospinning of thin PVDF fibers with preferred spatial arrangement and high polar phases content. Our preliminary cellular studies under in vitro conditions show that such nonwovens constitute promising smart scaffolds for tissue engineering applications, especially when stimulated by ultrasounds in order to activate their piezoelectric properties.

References

[1] T.E. Douglas, J. Schietse, A. Zima, S. Gorodzha, B.V. Parakhonskiy, D. Khalenkow, R. Shkarin, A. Ivanova, T. Baumbach, V. Weinhardt, Ch. Stevens, V. Vanhoorne, Ch. Vervaet, L. Balcaen, F. Vanhaecke, A. Slośarczyk, M. Surmaneva, R. Surmenev, and A. Skirtach, "Novel self-gelling injectable hydrogel/alpha-tricalcium phosphate composites for bone regeneration: Physiochemical and microcomputer tomographical characterization", *J. Biomed. Mater. Res. A*, 106(3), 822–828 (2018).

[2] B. Niemczyk, P. Sajkiewicz, and D. Kolbuk,"Injectable hydrogels as novel materials for central nervous system regeneration", *J. Neural Eng.* 15, 15 (2018).

[3] W. Matysiak, T. Tański, and M. Zaborowska, "Manufacturing process and characterization of electrospun PVP/ZnO NPs nanofibers", *Bull. Pol. Ac.: Tech.* 67(2), 193–200 (2019).

[4] B. Ostrowska, J. Jaroszewicz, E. Zaczynska, W. Tomaszewski, W. Swieszkowski, and K. Kurzydłowski, "Evaluation of 3D hybrid microfiber/nanofiber scaffolds for bone tissue engineering", *Bull. Pol. Ac.: Tech.* 62(3), 551–556 (2014).

[5] A. Ulatowska-Jarża, J. Pucińska, K. Wysocka-Król, I. Hołowacz, and H. Podbielska, "Nanotechnology for biomedical applications – enhancement of photodynamic activity by nanomaterials", *Bull. Pol. Ac.: Tech.* 59(3), 253–261 (2011).

[6] P. Sajkiewicz, "Crystallization behaviour of poly (vinylidene fluoride)", *Eur. Polym. J.* 35, 1581–1590 (1999).

[7] A. Gradys, P. Sajkiewicz, S. Adamovsky, A.A. Minakov, and C. Schick, "Crystallization of poly (vinylidene fluoride) during ultra-fast cooling", *Thermochimica Acta* 461, 153–157 (2007).

[8] A. Zaszczynska, P. Sajkiewicz, and A. Gradys, "Piezoelectric Scaffolds as Smart Materials for Neural Tissue Engineering", *Polymers*, 12(1), 161 (2020).

[9] Z.M. Dang, Y.H. Lin, and C.W. Nan, "Novel ferroelectric polymer composites with high dielectric constants". *Adv Mater* 15, 1625–1629 (2003).

[10] S. Yoon, A. Prabu, and K. Park, "Metal salt-induced ferroelectric crystalline phase in poly (vinylidene fluoride) films", *Macromol Rapid Commun* 29, 1316–1321 (2008).

[11] L. Yu and P. Cebe, "Crystal polymorphism in electrospun composite nanofibers of poly (vinylidene fluoride) with nanoclay", *Polymer*, 50, 2133–2141 (2009).

[12] T. Lei and L. Yu, Experiments and modelling of electrospinning process G. Zheng, "Electrospinning-induced preferred dipole orientation in PVDF fibers", *J Mater Sci* 50, 4342 (2015).

[13] T. Kowalewski and S. Błoński, Experiments and modelling of electrospinning process S. Baaral, „Experiments and modelling of electrospinning process", *Bull. Pol. Ac.: Tech*. 53(4), 385–394 (2005).

[14] A.J. Lovinger, "Annealing of poly (vinylidene fluoride) and formation of a fifth phase", *Macromolecules* 15, 40–44 (1982).

[15] R. Gregorio and M. Cestari, "Effect of crystallization temperature on the crystalline phase content and morphology of poly (vinylidene fluoride", *J. Polym. Sci. Part B Polym. Phys*. 32, 859–870 (1944).

[16] B. Bera and M. Sarkar, "Piezoelectricity in PVDF and PVDF Based Piezoelectric Nanogenerator: A Concept", *J Appl Phys* 9, 95–99 (2017).

[17] P. Sajkiewicz, A. Wasiak, and Z. Gocłowski, "Phase transitions during stretching of poly (vinylidene fluoride)", *European Polym. J.* 35(3), 423–429 (1999).

[18] K. Matsushige, K. Nagata, S. Imada, and T. Takemura, "The II-I crystal transformation of poly (vinylidene fluoride) under tensile and compressional stresses", *Polymer* 21, 1391–1397 (1980).

[19] J. Scheinbeim, C. Nakafuku, B.A. Newman, and K. Pae, "High-pressure crystallization of poly (vinylidene fluoride)", *J. Appl. Phys*., 50(6), 4399 – 4405 (1979).

[20] J. Wang, H. Li, J. Liu, Y. Duan, S. Jiang, and S. Yan, "On the α → β Transition of Carbon-Coated Highly Oriented PVDF Ultrathin Film Induced by Melt Recrystallization" *J Am Chem Soc.* 125(6), 1496–1497 (2003).

[21] Y. Ting, H. Gunawan, A. Sugondo, and Ch. Chiu, "A New Approach of Polyvinylidene Fluoride (PVDF) Poling Method for Higher Electric Response", *Ferroelectrics* 446, 28–38 (2013).

[22] S. Liang, Y. Kang, A. Tiraferri, E. Giannelis, H. Xia, and E. Menachem, "Highly Hydrophilic Polyvinylidene Fluoride (PVDF) Ultrafiltration Membranes via Postfabrication Grafting of Surface-Tailored Silica Nanoparticles", *ACS Appl Mater* 5(14), 6694–6703 (2013).

[23] D. Mandala, K. Henkelb, and D. Schmeißerb, "The electroactive β-phase formation in Poly (vinylidene fluoride) by gold nanoparticles doping", *Mater Lett* 73, 123–125 (2012).

[24] T.K. Sinha, S. Ghosh, R. Maiti, S. Jana, B. Adhikari, D. Mandal, and S.K. Ray, "Graphene-Silver-Induced Self-Polarized PVDF-Based Flexible Plasmonic Nanogenerator Toward the Realization for New Class of Self Powered Optical Sensor", *ACS Appl. Mater. Interfaces* 8(24), 14986–14993 (2016).

[25] A. Issa, M. Al-Maadeed, A. Luyt, D. Ponnamma, and M. Hassan, "Physico-Mechanical, Dielectric, and Piezoelectric Properties of PVDF Electrospun Mats Containing Silver Nanoparticles", *C—Journal of Carbon Research* 3(4), 30 (2017).

[26] F.A. He, K. Lin, D.L. Shi, H.L. Wu, H.K. Huang, J. Chen, F. Chen, and K.H. Lam, "Preparation of organosilicate/PVDF composites with enhanced piezoelectricity and pyroelectricity by stretching", *Compos Sci Technol* 137(12), 138–147 (2016).

[27] L. Jian-Hua, S. Xi-Sheng, Z. Qing, L. Mi-Zi, and Z. Qi-Qing, "The double effects of silver nanoparticles on the PVDF membrane: Surface hydrophilicity and antifouling performance", *Appl Surf Sci*. 265, 663–670 (2013).

[28] J. Sakata and M. Mochizuki, "Preparation of organic thin films by an electrospray technique I. Crystal forms and their orientation in poly (vinylidene flouride) films", *Thin Solid Films* 195, 175–184 (1991).

[29] S. Damaraju, S. Wu, M. Jaffe, and T. Arinzeh, "Structural changes in PVDF fibers due to electrospinning and its effect on biological function", *Biomed. Mater.* 8, 045007 (2013).

[30] C. Ribeiro, J. Pärssinen, V. Sencadas, V. Correia, S. Miettinen, V. Hytönen, and S. Lanceros-Méndez, "Dynamic piezoelectric stimulation enhances osteogenic differentiation of human adipose stem cells", *J. Biomed. Mater. Res.* 103, 2172–2175 (2014).

[31] M.T. Rodrigues, M.E. Gomes, J.F. Mano, and R.L. Reis, „β-PVDF Membranes Induce Cellular Proliferation and Differentiation in Static and Dynamic Conditions", *Materials Science Forum* 587–588, 72–76 (2008).

[32] M. Hoop, X.Z. Chen, A. Ferrari, F. Mushtaq, G. Ghazaryan, T. Tervoort, D. Poulikakos, B. Nelson, and S. Pané, "Ultrasound-mediated piezoelectric differentiation of neuron-like PC12 cells on PVDF membranes", *Scientific Reports* 7, 4028 (2017).

[33] L. Ghasemi-Mobarakeh, M.P. Prabhakaran, M. Morshed, M. Hossein, N.E. Hossein, B.S. Kiani, S. Al-Deyab, and S. Ramakrishna,"Application of conductive polymers, scaffolds and electrical stimulation for nerve tissue engineering", *J Tissue Eng Regen M* (2017).

[34] A.G. Kolbeck, „Aging of piezoelectricity in poly (vinylidene fluoride)", *J Polym Sci Pol Phys.* 20, 1987–2001 (1982).

[35] S.B. Rodan, Y. Imai, M.A. Thiede, G. Wesolowski, D. Thompson, Z. Bar-Shavit, S. Shull, K. Mann, and G.A. Rodan, "Characterization of a Human Osteosarcoma Cell Line (Saos-2) with Osteoblastic Properties", *Cancer Res*. 47, 4961–4966 (1987).

[36] D. Klee, Z. Ademovic, A. Bosserhoff, H. Hoecker, G. Maziolis, and H.J. Erli, "Surface modification of poly (vinylidenefluoride) to improve the osteoblast adhesio", *Biomaterials* 24, 3663–3670 (2003).

[37] W.A. Yeea, M. Kotaki, Y. Liu, and X. Lu, "Morphology, polymorphism behavior and molecular orientation of electrospun poly (vinylidene fluoride) fibers", *Polymer* 48(2), 512–521 (2007).

[38] Y. Li, Ch. Liao, and S.Ch. Tjong, "Electrospun Polyvinylidene Fluoride-Based Fibrous Scaffolds with Piezoelectric Characteristics for Bone and Neural Tissue Engineering", *Nanomaterials* (Basel) 9(7), 952 (2019).

[39] X. Cai, T. Lei, D. Sund, and L. Linde, "A critical analysis of the a, b and g phases in poly (vinylidene fluoride) using FTIR", *RSC Adv*. 7, 15382–15389 (2017).

[40] K. Chwee and T. Limbc, "Nanofiber technology: current status and emerging developments", *Prog Polym Sci.* 70, 1–17 (2017).

[41] Z.M. Huang, Y.Z. Zhang, M. Kotaki, and S. Ramakrishna, "A review on polymernanofibers by electrospinning and their applications in nanocomposites", *Compos. Sci. Technol*. 63(15), 2223–2253 (2003).

[42] E. Zussman, A. Theron, and A. Yarin, "Formation of nanofiber crossbars in electrospinning", *Appl. Phys. Lett.* 82(6), 973–975 (2003).

[43] H. Pan, L. Li, L. Hu, and X. Cui, "Continuous aligned polymer fibers produced by a modified electrospinning method", *Polymer* 47(14), 4901–4904 (2006).

[44] B. Sundaray, V. Subramanian, T. Natarajan, R.Z. Xiang, C.C. Chang, and W.S. Fann, "Electrospinning of continuous aligned polymer fibers", *Appl. Phys. Lett*. 84(7), 1222–1224 (2004).